

Nonlinear Motion Control of Mobile Robot Dynamic Model

Jasmin Velagic, Bakir Lacevic and Nedim Osmic
*University of Sarajevo
Bosnia and Herzegovina*

1. Introduction

The problem of motion planning and control of mobile robots has attracted the interest of researchers in view of its theoretical challenges because of their obvious relevance in applications. From a control viewpoint, the peculiar nature of nonholonomic kinematics and dynamic complexity of the mobile robot makes that feedback stabilization at a given posture cannot be achieved via smooth time-invariant control (Oriolo et al., 2002). This indicates that the problem is truly nonlinear; linear control is ineffective, and innovative design techniques are needed.

In recent years, a lot of interest has been devoted to the stabilization and tracking of mobile robots. In the field of mobile robotics, it is an accepted practice to work with dynamical models to obtain stable motion control laws for trajectory following or goal reaching (Fierro & Lewis, 1997). In the case of control of a dynamic model of mobile robots authors usually used linear and angular velocities of the robot (Fierro & Lewis, 1997; Fukao et al., 2000) or torques (Rajagopalan & Barakat, 1997; Topalov et al., 1998) as an input control vector. The central problem in this paper is reduction of control torques during the reference position tracking. In the case of dynamic mobile robot model, the position control law ought to be nonlinear in order to ensure the stability of the error that is its convergence to zero (Oriolo et al., 2002). The most authors solved the problem of mobile robot stability using nonlinear backstepping algorithm (Tanner & Kyriakopoulos, 2003) with constant parameters (Fierro & Lewis, 1997), or with the known functions (Oriolo et al., 2002). In (Tanner & Kyriakopoulos, 2003) a combined kinematic/torque controller law is developed using backstepping algorithm and stability is guaranteed by Lyapunov theory. In (Oriolo et al., 2002) method for solving trajectory tracking as well as posture stabilization problems, based on the unifying framework of dynamic feedback linearization was presented.

The objective of this chapter is to present advanced nonlinear control methods for solving trajectory tracking as well as convergence of stability conditions. For these purposes we developed a backstepping (Velagic et al., 2006) and fuzzy logic position controllers (Lacevic, et al., 2007). It is important to note that optimal parameters of both controllers are adjusted using genetic algorithms. The novelty of this evolutionary approach lies in automatic obtaining of suboptimal set of control parameters which differs from standard manual adjustment presented in (Hu & Yang, 2001; Oriolo et al., 2002). The considered motion control system of the mobile robot has two levels. The lower level subsystem deals with the

control of linear and angular velocities using a multivariable PI controller described with a full matrix. This torque control ensures tracking servo inputs with zero steady state errors (Velagic et al., 2005). The position control of the mobile robot is a nonlinear and it is on the second level. We have developed a mobile robot position controller based on backstepping control algorithm with the extension to rapidly decrease the control torques needed to achieve the desired position and orientation of mobile robot (Lacevic & Velagic, 2005). This is important in the case if the initial position of reference robot does not belong to the straight line, determined with the robot and its initial orientation. Also, we have designed a fuzzy logic position controller whose membership functions are tuned by genetic algorithm (Lacevic, et al., 2007). The main goals are to ensure both successfully velocity and position trajectories tracking between the mobile robot and the reference cart. The proposed fuzzy controller has two inputs and two outputs. The first input represents the distance between the mobile robot and the reference cart. The second input is the angle formed by the straight line defined with the orientation of the robot, and the straight line that connects the robot with the reference cart. Outputs represent linear and angular velocity inputs, respectively. The performance of proposed systems is investigated using a dynamic model of a nonholonomic mobile robot with the friction considered. The quality of the fuzzy controller is analyzed through comparison with previously developed a mobile robot position controller based on backstepping control algorithm. Simulation results indicated good quality of both position tracking and torque capabilities with the proposed fuzzy controller. Also, noticeable improvement of torques reduction is achieved in the case of fuzzy controller.

2. Control system topology

The proposed control system with two-level controls is shown in Fig. 1. The low level velocity control system is composed of a multivariable PI controller and dynamic model of mobile robots and actuators. The medium level position control system generates a nonlinear control law whose parameters are obtained using a genetic algorithm.

In the following sections the design of the control system blocks from Fig. 1 is described.

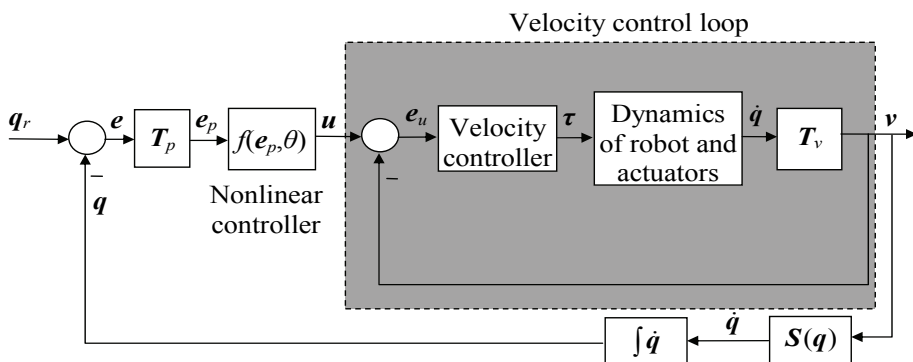


Figure 1. Mobile robot position and velocity control

2.1 Dynamics of mobile robot

In this section, a dynamic model of a nonholonomic mobile robot with the viscous friction will be derived first. A typical representation of a nonholonomic mobile robot is shown in Fig. 2.

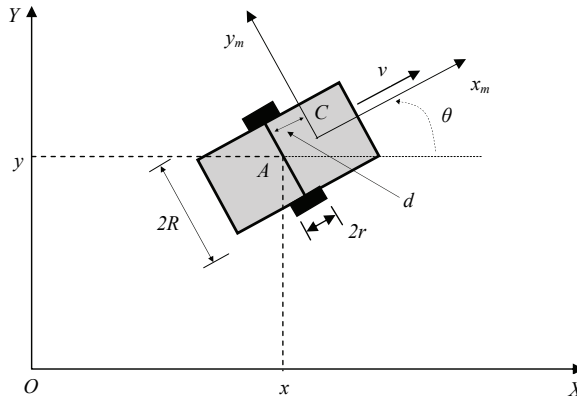


Figure 2. The representation of a nonholonomic mobile robot

The robot has two driving wheels mounted on the same axis and a free front wheel. Two driving wheels are independently driven by two actuators to achieve both the transition and orientation. The position of the mobile robot in the global frame $\{X, O, Y\}$ can be defined by the position of the mass center of the mobile robot system, denoted by C , or alternatively by position A , which is the center of mobile robot gear, and the angle between robot local frame $\{x_m, C, y_m\}$ and global frame. The kinetic energy of the whole structure is given by the following equation:

$$T = T_l + T_r + T_{kr} \tag{1}$$

where T_l is a kinetic energy that is consequence of pure translation of the entire vehicle, T_r is a kinetic energy of rotation of the vehicle in XOY plane, and T_{kr} is the kinetic energy of rotation of wheels and rotors of DC motors. The values of introduced energy terms can be expressed by Eqs. (2)-(4):

$$T_l = \frac{1}{2} M v_c^2 = \frac{1}{2} M (\dot{x}_c^2 + \dot{y}_c^2) \tag{2}$$

$$T_r = \frac{1}{2} I_A \dot{\theta}^2 \tag{3}$$

$$T_{kr} = \frac{1}{2} I_0 \dot{\theta}_R^2 + \frac{1}{2} I_0 \dot{\theta}_L^2 \tag{4}$$

where M is the mass of the entire vehicle, v_c is linear velocity of the vehicle's center of mass C , I_A is the moment of inertia of the entire vehicle considering point A , θ is the angle that represents the orientation of the vehicle (Fig. 2), I_0 is the moment of inertia of the rotor/wheel complex and $d\theta_R/dt$ and $d\theta_L/dt$ are angular velocities of the right and left wheel respectively.

Further, the components of the velocity of the point A , can be expressed in terms of $d\theta_R/dt$ and $d\theta_L/dt$:

$$\dot{x}_A = \frac{r}{2}(\dot{\theta}_R + \dot{\theta}_L) \cos \theta, \quad (5)$$

$$\dot{y}_A = \frac{r}{2}(\dot{\theta}_R + \dot{\theta}_L) \sin \theta, \quad (6)$$

$$\dot{\theta} = \frac{r(\dot{\theta}_R - \dot{\theta}_L)}{2R}. \quad (7)$$

Since $\dot{x}_C = \dot{x}_A - d\dot{\theta} \sin \theta$ and $\dot{y}_C = \dot{y}_A + d\dot{\theta} \cos \theta$, where d is distance between points A and C , it is obvious that following equations follow:

$$\dot{x}_C = \frac{r}{2}(\dot{\theta}_R + \dot{\theta}_L) \cos \theta - d\dot{\theta} \sin \theta, \quad (8)$$

$$\dot{y}_C = \frac{r}{2}(\dot{\theta}_R + \dot{\theta}_L) \sin \theta + d\dot{\theta} \cos \theta. \quad (9)$$

By substituting terms in (1) with expressions in equations (2)-(9), total kinetic energy of the vehicle can be calculated in terms of $d\theta_R/dt$ and $d\theta_L/dt$:

$$T(\dot{\theta}_R, \dot{\theta}_L) = \left(\frac{Mr^2}{8} + \frac{(I_A + Md^2)r^2}{8R^2} + \frac{I_0}{2} \right) \dot{\theta}_R^2 + \left(\frac{Mr^2}{8} + \frac{(I_A + Md^2)r^2}{8R^2} + \frac{I_0}{2} \right) \dot{\theta}_L^2 + \left(\frac{Mr^2}{4} - \frac{(I_A + Md^2)r^2}{4R^2} \right) \dot{\theta}_R \dot{\theta}_L \quad (10)$$

Now, the Lagrange equations:

$$\frac{d}{dt} \left(\frac{\partial L}{\partial \dot{\theta}_R} \right) - \frac{\partial L}{\partial \theta_R} = \tau_R - K \dot{\theta}_R, \quad (11)$$

$$\frac{d}{dt} \left(\frac{\partial L}{\partial \dot{\theta}_L} \right) - \frac{\partial L}{\partial \theta_L} = \tau_L - K \dot{\theta}_L, \quad (12)$$

are applied.

Here τ_R and τ_L are right and left actuation torques and $Kd\theta_R/dt$ and $Kd\theta_L/dt$ are the viscous friction torques of right and left wheel-motor systems, respectively.

Finally, the dynamic equations of motion can be expressed as:

$$A \ddot{\theta}_R + B \ddot{\theta}_L = \tau_R - K \dot{\theta}_R, \quad (13)$$

$$B \ddot{\theta}_R + A \ddot{\theta}_L = \tau_L - K \dot{\theta}_L, \quad (14)$$

where

$$A = \left(\frac{Mr^2}{4} + \frac{(I_A + Md^2)r^2}{4R^2} + I_0 \right) \quad (15)$$

$$B = \left(\frac{Mr^2}{4} - \frac{(I_A + Md^2)r^2}{4R^2} \right)$$

In this chapter we used a mobile robot with the following parameters: $M=10\text{kg}$, $I_A=1\text{kgm}^2$, $r=0.035\text{ m}$, $R=0.175\text{ m}$, $d=0.05\text{ m}$, $m_0=0.2\text{ kg}$, $I_0=0.001\text{ kgm}^2$ and $K/A=0.5$.

In the following section a design of both velocity and position controls will be established.

2.2. Velocity control of mobile robot

The dynamics of the velocity controller is given by the following equations in Laplace domain:

$$\tau(s) = \begin{bmatrix} \tau_R(s) \\ \tau_L(s) \end{bmatrix} = \frac{1}{r} \begin{bmatrix} g_1(s) & g_2(s) \\ g_1(s) & -g_2(s) \end{bmatrix} \begin{bmatrix} e_v(s) \\ e_\omega(s) \end{bmatrix}, \tag{16}$$

where $e_v(s)$ is the linear velocity error, and $e_\omega(s)$ is the angular velocity error. This structure differs from previously used diagonal structures. Transfer functions $g_j(s)$ are chosen to represent PI controllers:

$$g_1(s) = K_1 \left(1 + \frac{1}{T_{i1}s}\right) \cdot R, \quad g_2(s) = K_2 \left(1 + \frac{1}{T_{i2}s}\right) \cdot R. \tag{17}$$

The particular choice of the adopted multivariable PI controller described by equations (16) and (17) is justified with the following theorem.

Theorem 1. Torque control (16) ensures tracking servo inputs u_1 and u_2 with zero steady state errors.

Proof: When we substitute $\dot{\theta}_R$ with ω_R , $\dot{\theta}_L$ with ω_L , and consider (16), we can write another form of (13) and (14):

$$\begin{bmatrix} As+K & Bs \\ Bs & As+K \end{bmatrix} \begin{bmatrix} \omega_R(s) \\ \omega_L(s) \end{bmatrix} = \frac{1}{r} \begin{bmatrix} g_1(s) & g_2(s) \\ g_1(s) & -g_2(s) \end{bmatrix} \begin{bmatrix} u_1(s) - v(s) \\ u_2(s) - \omega(s) \end{bmatrix}, \tag{18}$$

ω_R and ω_L can be expressed in terms of ω and v as:

$$\omega_R = \frac{v + R\omega}{r}, \quad \omega_L = \frac{v - R\omega}{r}. \tag{19}$$

Then, equation (18) can be transformed to:

$$\begin{bmatrix} As+K & Bs \\ Bs & As+K \end{bmatrix} \begin{bmatrix} v(s) + R\omega(s) \\ v(s) - R\omega(s) \end{bmatrix} = \begin{bmatrix} g_1(s) & g_2(s) \\ g_1(s) & -g_2(s) \end{bmatrix} \begin{bmatrix} u_1(s) - v(s) \\ u_2(s) - \omega(s) \end{bmatrix},$$

and further to:

$$\begin{bmatrix} \alpha_1(s) & \alpha_2(s) \\ \alpha_1(s) & -\alpha_2(s) \end{bmatrix} \begin{bmatrix} v(s) \\ \omega(s) \end{bmatrix} = \begin{bmatrix} g_1(s) & g_2(s) \\ g_1(s) & -g_2(s) \end{bmatrix} \begin{bmatrix} u_1(s) \\ u_2(s) \end{bmatrix}, \tag{20}$$

where

$$\alpha_1(s) = \frac{(A+B)s^2 + (K + K_1T_{i1})s + K_1}{s}$$

$$\alpha_2(s) = \frac{R(A-B)s^2 + (RK + K_2T_{i2})s + K_2}{s}. \tag{21}$$

Following equations could be easily derived from (20):

$$\begin{aligned} v(s) &= \frac{g_1}{\alpha_1} u_1(s) = G_1 u_1(s) = \frac{K_1 T_{i1} s + K_1}{(A+B)s^2 + (K + K_1 T_{i1})s + K_1} u_1(s) \\ \omega(s) &= \frac{g_2}{\alpha_2} u_2(s) = G_2 u_2(s) = \frac{K_2 T_{i2} s + K_2}{R(A-B)s^2 + (RK + K_2 T_{i2})s + K_2} u_2(s) \end{aligned} \quad (22)$$

It is obvious that transfer functions G_1 and G_2 are static with gains equal to "1", which completes the **proof**.

The velocity control loop structure is shown in Fig. 1, as an inner loop. From the simulation results obtained (Figs. 3 and 4), it can be seen that the proposed PI controller successfully tracks the given linear and angular velocity profiles.

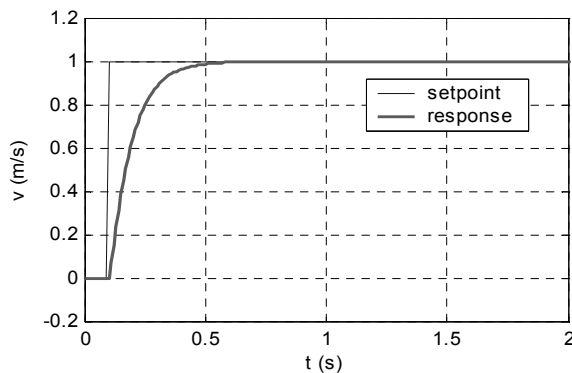


Figure 3. Linear velocity step response

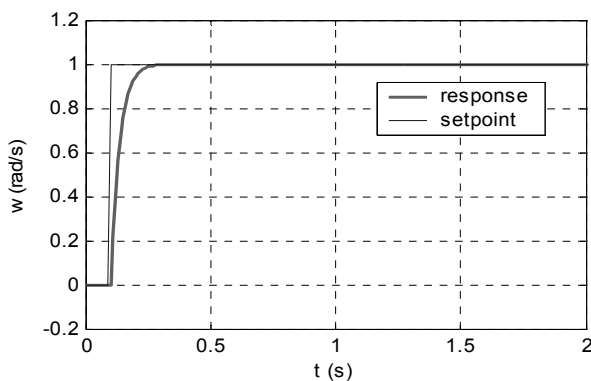


Figure 4. Angular velocity step response

The controller parameters used for this simulation are $K_1=129.7749$, $K_2=41.0233$, $T_{i1}=11.4018$, $T_{i2}=24.1873$, which are tuned using standard GA.

The design of position controls of mobile robot, backstepping and fuzzy logic controllers, will be described in the next section.

3. Position control of mobile robot

The trajectory position tracking problem for a mobile robot is formulated with the introduction of a virtual reference robot to be tracked (Egerstedt et al., 2001) (Fig. 5). The tracking position error between the reference robot and the actual robot can be expressed in the robot frame as:

$$e_p = \begin{bmatrix} e_1 \\ e_2 \\ e_3 \end{bmatrix} = T_p e_q = \begin{bmatrix} \cos \theta & \sin \theta & 0 \\ -\sin \theta & \cos \theta & 0 \\ 0 & 0 & 1 \end{bmatrix} \begin{bmatrix} x_r - x \\ y_r - y \\ \theta_r - \theta \end{bmatrix}, \tag{23}$$

where $e_q = [e_x \ e_y \ e_\theta]^T$.

The position error dynamics can be obtained from the time derivative of the (23) as:

$$\dot{e}_1 = \omega e_2 + u_1, \quad \dot{e}_2 = -\omega e_1 + v, \sin e_3, \quad \dot{e}_3 = u_2, \tag{24}$$

where $v = v_r \cos e_3 - u_1$ and $\omega = \omega_r - u_2$.

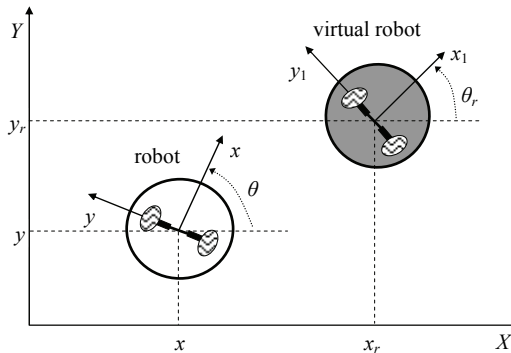


Figure 5. The concept of tracking of a virtual reference robot

3.1. Backstepping controller design

In paper (Lacevic & Velagic, 2006) we proposed the following position control law that ensures stability

$$\begin{aligned} u_1 &= -\alpha p e_1 \cdot f(\mathbf{x}) \\ u_2 &= -\frac{2\alpha p}{q} (e_1^2 + e_2^2)^{\alpha-1} v_r e_2 - q \sin e_3 \cdot g(\mathbf{x})' \end{aligned} \tag{25}$$

where p and q are positive real constants, and $a > 1$ and $f(x)$ and $g(x)$ are functions of some vector $x \in \mathbf{R}^m$, $m \in \mathbf{N}$, satisfying the condition: $\exists L > 0: f(x), g(x) \geq L, \forall x \in \mathbf{R}^m$.

Our theorem which proved this statement is derived as follows.

Theorem 2. Control law, given in (25), provides stability of the mobile robot model, respect to the reference trajectory (i.e., $\lim_{t \rightarrow \infty} (e_1^2(t) + e_2^2(t)) = 0 \wedge \lim_{t \rightarrow \infty} e_3(t) = k\pi, k \in \mathbf{Z}$).

Proof:

Consider the Lyapunov function candidate:

$$V(e_1, e_2, e_3) = p(e_1^2 + e_2^2)^\alpha + q(1 - \cos(e_3)). \quad (26)$$

Deriving (26), and using the expressions from error dynamics (24), we obtain:

$$\begin{aligned} \dot{V}(e_1, e_2, e_3) = & 2\alpha p(e_1^2 + e_2^2)^{\alpha-1} u_1 + (q \sin e_3) u_2 \\ & + 2\alpha p(e_1^2 + e_2^2)^{\alpha-1} e_2 v_r \sin e_3 \end{aligned} \quad (27)$$

Substituting u_1 and u_2 from (25) we get:

$$\begin{aligned} \dot{V}(e_1, e_2, e_3) = & -2\alpha^2 p^2 e_1^2 (e_1^2 + e_2^2)^{\alpha-1} \cdot f(\mathbf{x}) \\ & - q^2 (\sin^2 e_3) \cdot g(\mathbf{x}) < 0 \end{aligned} \quad (28)$$

Thus, function $\dot{V}(e_1, e_2, e_3)$ is uniformly continuous, $V(e_1, e_2, e_3)$ tends to some positive finite value and $\|e_p(t)\|$ is bounded. Using Barbalat lemma, $\dot{V}(e_1, e_2, e_3)$ tends to zero. From (28), it is obvious that $\lim_{t \rightarrow \infty} e_1(t) = 0$ and $\lim_{t \rightarrow \infty} e_3(t) = k\pi$, $k \in \mathbb{Z}$. Further, it is clear that $\lim_{t \rightarrow \infty} \dot{e}_3(t) = 0$, and hence (using (24)) $\lim_{t \rightarrow \infty} u_2 = 0$. From the expression for u_2 in (25) one can conclude that $\lim_{t \rightarrow \infty} e_2(t) = 0$.

The ‘‘obstacle’’ for global asymptotical stability of the system is the lack of guarantee that the error e_3 will converge to zero. In the worst case scenario, the robot will track the reference cart by moving backwards. This behaviour however, was not observed in any of case studies.

The parameters of both velocity and position controllers are encoded into binary chromosome (here, functions f and g are assumed as constants) is shown in Fig. 6. Each parameter is presented with 12 bits. Each individual was assigned an objective value, based on the following functional:

$$F = \sum_{i=1}^3 \left[a_i \int_0^{t_s} \ln(1 + |e_i(t)|) dt \right] + a_R \cdot \max_{t \in [0, t_s]}(\tau_R(t)) + a_L \cdot \max_{t \in [0, t_s]}(\tau_L(t)), \quad (29)$$

where

$$a_1 = 1, a_2 = 5, a_3 = 1, t_s = 16, a_R = a_L = 1.$$

It is obvious that the better individual has smaller value of F . The second part of the expression represents penalty for the great values of control torques. The objective value for each individual is evaluated upon the simulation run that includes the tracking of reference trifolium trajectory (Figures in simulation results section).

Simple GA with population size 51, tournament selection, uniform crossover, bit mutation, and elitism has been used.

Evolution yielded following values:

$$p = 1.9934, q = 0.0530, f = 9.8615, g = 2.9956, K_1 = 128.444, Ti_1 = 60.9756, K_2 = 29.048, Ti_2 = 31.4465.$$

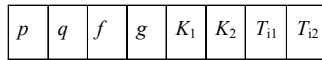


Figure 6. Mapping the set of tunable parameters into chromosome

It has been noticed, that, at the beginning of tracking, the control torques increase rapidly if the initial position of reference robot does not belong to the straight line, determined with the robot and its initial orientation (Lacevic and Velagic, 2005) (Fig. 7).

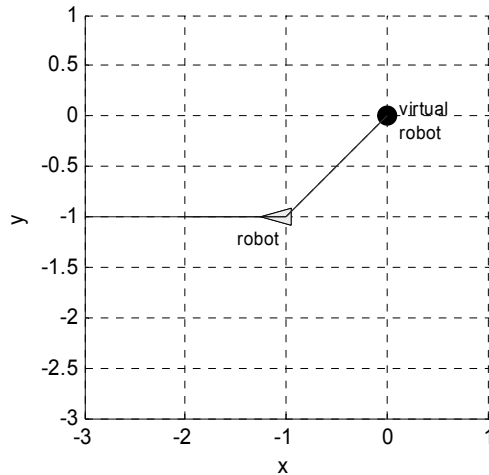


Figure 7. Tracking robot doesn't "see" virtual robot

3.2. Hybrid backstepping controller design

For improving the mentioned weakness a hybrid backstepping position controller is designed. For that purpose, the following control law, which provides velocity servo inputs, is proposed (Lacevic & Velagic, 2005):

$$\begin{aligned} \bar{u}_1(t) &= \alpha(t)u_1(t) \\ \bar{u}_2(t) &= \alpha(t)u_2(t) + (1 - \alpha(t))\omega_s(t) \end{aligned} \tag{30}$$

Function $\omega_s(t)$ is produced, as the output of the following system (Fig. 8).

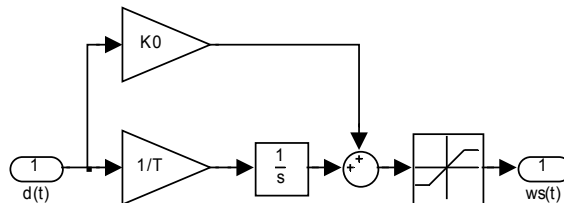


Figure 8. Producing $\omega_s(t)$

The function $d(t)$ is given with:

$$d(t) = \text{sgn}(\text{atan2}(e_y(t), e_x(t)) - \theta(t)). \quad (31)$$

Function $a(t)$ is determined with the following differential equation:

$$b_0 \frac{d^2 \alpha(t)}{dt^2} + b_1 \frac{d \alpha(t)}{dt} + \alpha(t) = z(t), \quad (32)$$

where $z(t)$ is practically a step function given with:

$$z(t) = \begin{cases} 1, & \text{if } \exists t_1 \in [0, t] : \theta(t_1) = \text{atan2}(e_y(t_1), e_x(t_1)), \\ 0, & \text{otherwise} \end{cases}, \quad (33)$$

This way, the robot doesn't start tracking virtual robot instantly; it first rotates around its own axis with increasing angular velocity $\omega_s(t)$, until it "sees" the virtual robot (Fig. 9).

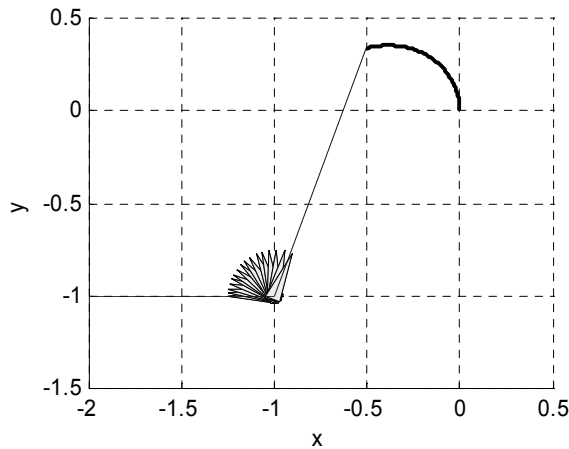


Figure 9. "Seeking" a virtual robot

In the next subsection the design procedure of proposed fuzzy position controller will be described.

3.3. Design of fuzzy controller

In order to reduce the control torques and velocity inputs, fuzzy position controller is designed. Fuzzy system based on Sugeno inference model with 2 inputs and 2 outputs is used instead of classical backstepping controller (Fig. 10).

Inputs i_1 and i_2 are following signals:

$$i_1 = \sqrt{e_1^2 + e_2^2} = \sqrt{e_x^2 + e_y^2}, \quad i_2 = f(\text{atan2}(e_y, e_x) - \theta), \quad (34)$$

where f is given with:

$$f(x) = 2 \operatorname{atan} \left(\tan \left(\frac{x}{2} \right) \right). \tag{35}$$

Input i_1 represents the distance between the mobile robot and the reference cart. Input i_2 is the angle formed by the straight line defined with the orientation of the robot, and the straight line that connects the robot with the reference cart. Function f ensures that variable i_2 belongs to the interval $(-\pi, \pi]$ (Fig. 11). Outputs o_1 and o_2 represent linear and angular velocity inputs respectively.

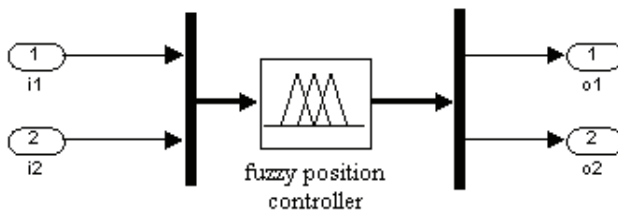


Figure 10. Fuzzy controller with 2 inputs and 2 outputs

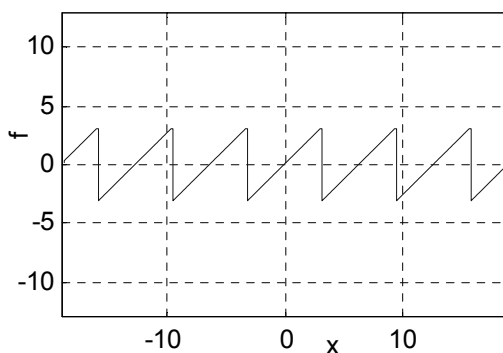


Figure 11. Diagram of the function f

Inputs i_1 and i_2 will be modeled with two trapezoidal and five triangular shape membership functions, respectively. Random initial setups of mentioned variables are shown in Figs. 12 and 13. The parameters of input variables are (a_1) and $(b_1, b_2, b_3, b_4, b_5 \text{ i } b_6)$. Outputs o_1 and o_2 are represented by singleton functions with five and three membership values (Figs. 14 and 15). These outputs are described with parameters $(c_1, c_2, c_3, c_4 \text{ and } c_5)$ and $(d_1, d_2 \text{ and } d_3)$, respectively. Parameters a_i, b_i, c_i and d_i that determine the membership functions are encoded into binary chromosome in Fig 16 (the same as in a previously described algorithm), while the rules set remained invariant during the GA run. Parameters of velocity controller kept their values, obtained previously.

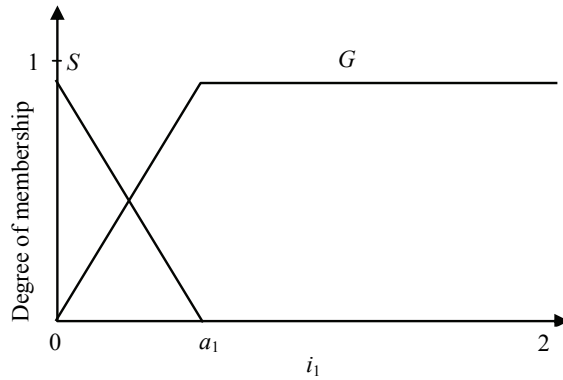


Figure 12. Random initial setup of input variable i_1

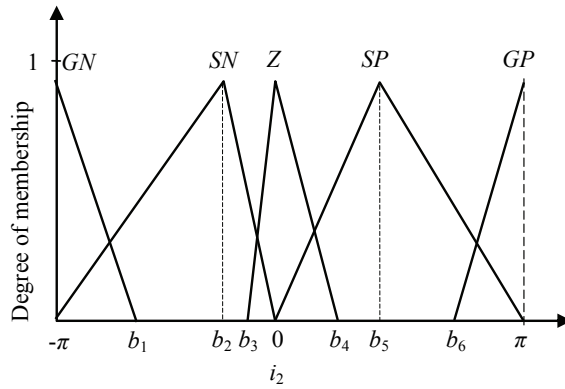


Figure 13. Random initial setup of input variable i_2

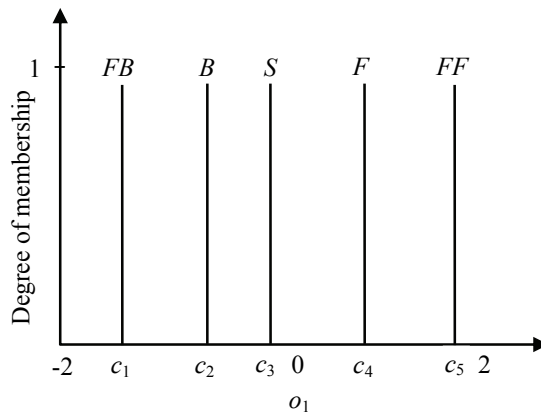


Figure 14. Random initial setup of output variable o_1

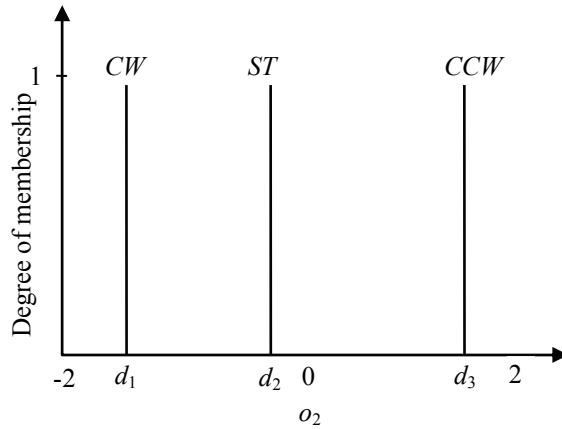


Figure 15. Random initial setup of output variable o_2

a_1	b_1	b_2	b_3	b_4	b_5	b_6	c_1	c_2	c_3	c_4	c_5	d_1	d_2	d_3
-------	-------	-------	-------	-------	-------	-------	-------	-------	-------	-------	-------	-------	-------	-------

Figure 16. Representation of binary chromosome of parameters

Finally, the rules that complete the inference model are:

- If (i_1 is S) and (i_2 is GN) then (o_1 is B) (o_2 is CW)
- If (i_1 is S) and (i_2 is SN) then (o_1 is F) (o_2 is CW)
- If (i_1 is S) and (i_2 is Z) then (o_1 is S) (o_2 is ST)
- If (i_1 is S) and (i_2 is SP) then (o_1 is F) (o_2 is CCW)
- If (i_1 is S) and (i_2 is GP) then (o_1 is B) (o_2 is CCW)
- If (i_1 is G) and (i_2 is GN) then (o_1 is FB) (o_2 is CW)
- If (i_1 is G) and (i_2 is SN) then (o_1 is FF) (o_2 is CW)
- If (i_1 is G) and (i_2 is Z) then (o_1 is FF) (o_2 is ST)
- If (i_1 is G) and (i_2 is SP) then (o_1 is FF) (o_2 is CCW)
- If (i_1 is G) and (i_2 is GP) then (o_1 is FB) (o_2 is CCW)

Evolution of membership functions parameters is performed by identical way as in the case of backstepping controller design (subsection 3.1). The GA with population size 101, tournament selection, uniform crossover, bit mutation, and elitism has been used. Also, the objective function is same as in (29). Resulting membership functions for input and output variables are shown in Figs. 17-20.

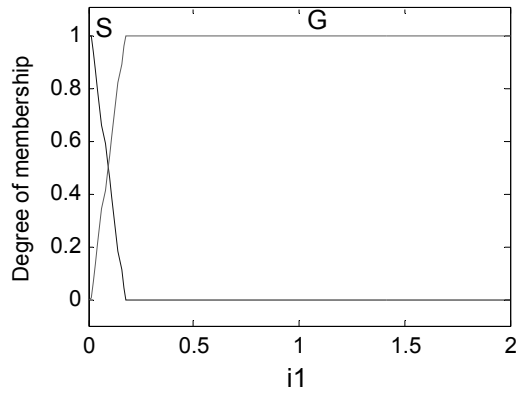


Figure 17. Membership functions for i_1

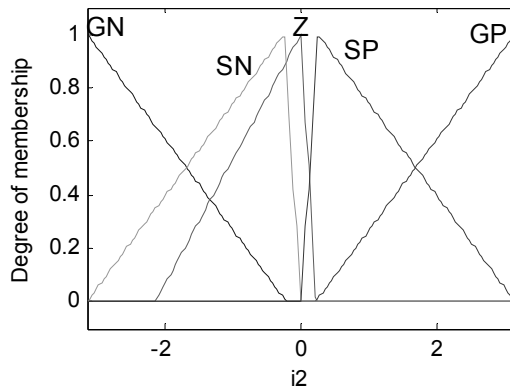


Figure 18. Membership functions for i_2

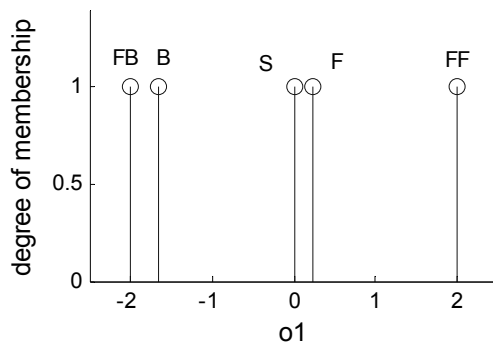


Figure 19. Membership functions for o_1 (fast backwards, backwards, stop, forward and fast forward)

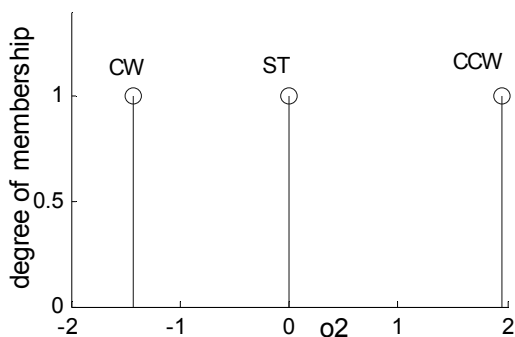


Figure 20. Membership functions for ω_2 (clockwise, straight, counter clockwise)

Important characteristic of this controller is that its outputs are inherently limited. Disadvantage of this concept lies in its inability to ensure tracking of the reference cart that has velocities which are bigger than those that fuzzy controller can "suggest". Advantage lies in the fact that control velocities (and consequently, the control torques) cannot exceed certain limits (see simulation results in the next section). Resulting control surfaces are shown in Figs. 21 and 22.

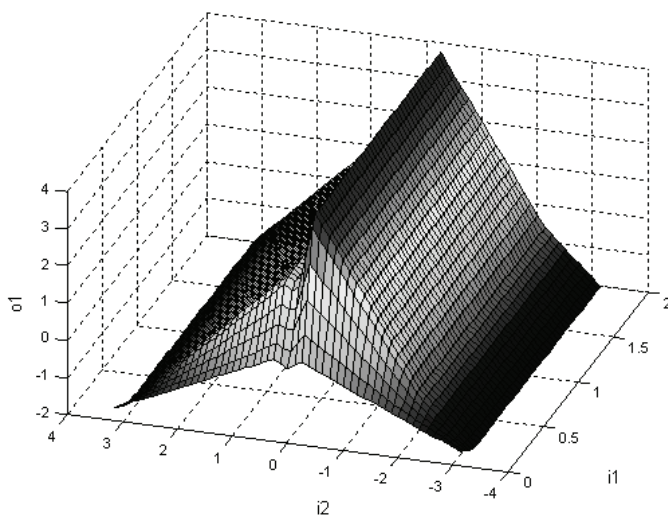


Figure 21. Control surface for ω_1

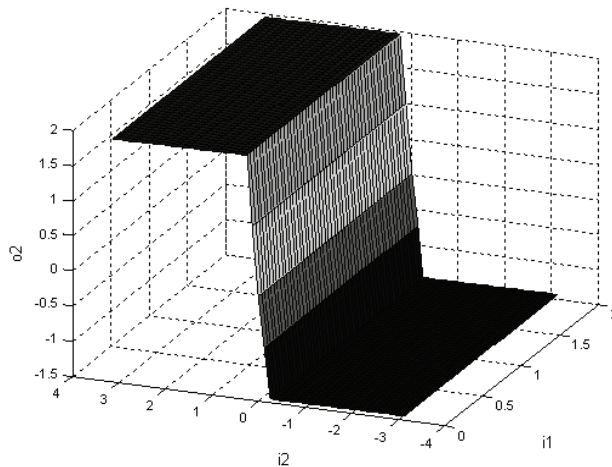


Figure 22. Control surface for o_2

4. Simulation results

The validation of proposed fuzzy controller will be tested in the comparison with backstepping control algorithm. The effectiveness of the both controllers is demonstrated in the case of tracking of a lamniscate and trifolium curves. The overall system is designed and implemented within Matlab/Simulink environment. We consider the following profiles: position, orientation, linear and angular velocities and torques.

4.1 Simulation results with backstepping controllers

The control performance of the ordinary and hybrid backstepping controllers will be illustrated in this subsection through their comparative analysis. The simulation results obtained are shown in Figs. 23-26.

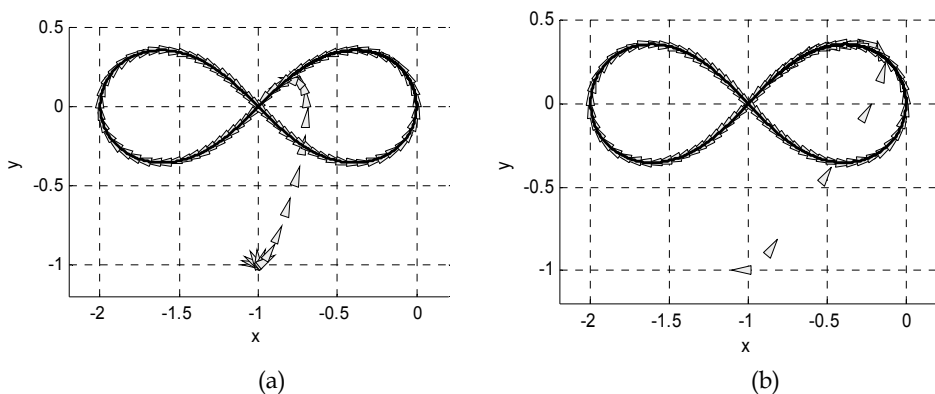


Figure 23. Tracking a lemniscate trajectory with (a) hybrid and (b) ordinary controllers

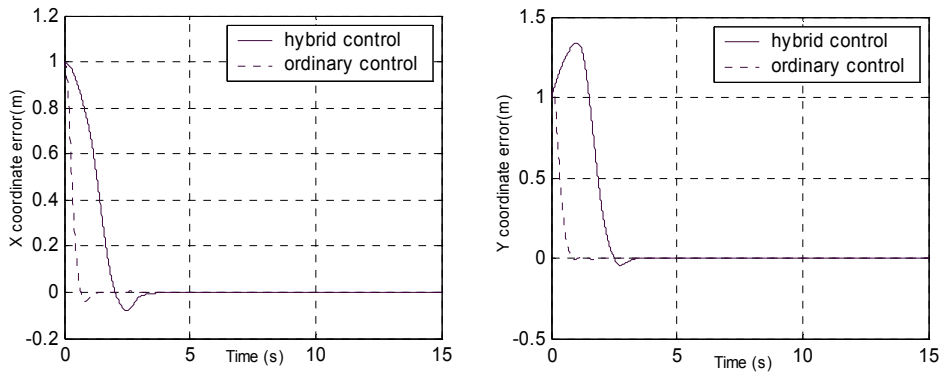


Figure 24. X and Y coordinate errors

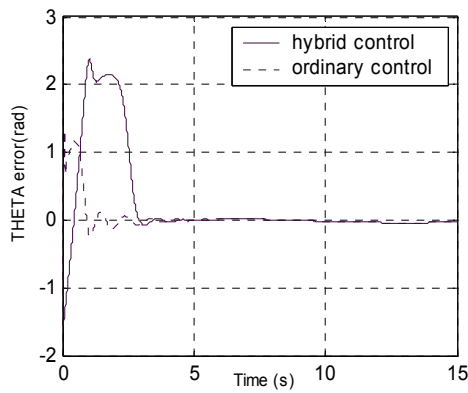


Figure 25. Orientation error

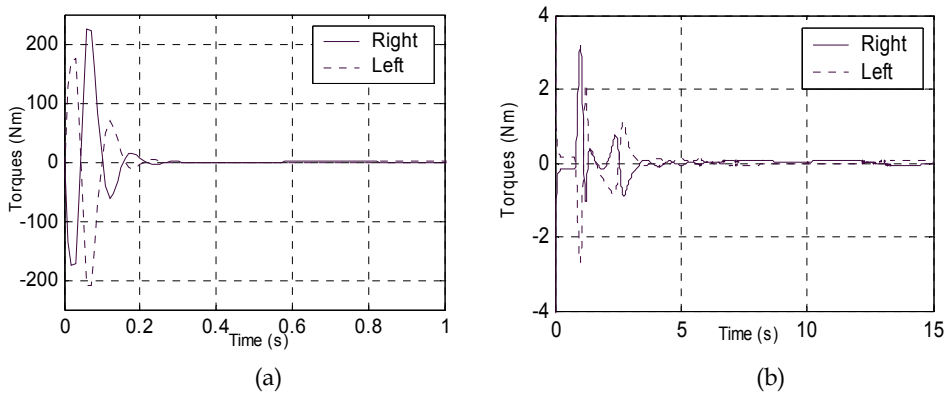
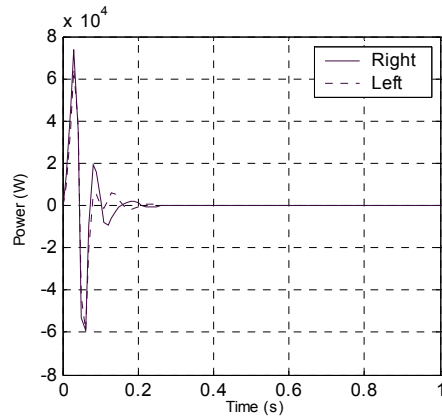
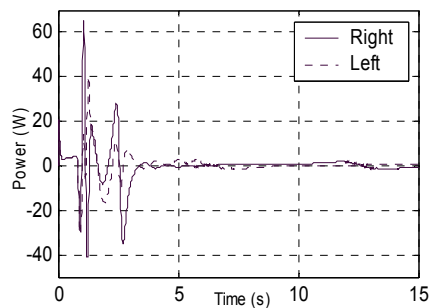


Figure 26. Control torques of ordinary (a) and hybrid (b) backstepping controllers



(a)



(b)

Figure 26. Requested power of DC motors: (a) hybrid and (b) ordinary backstepping controllers (ordinary controller - the first second of tracking)

These results demonstrate the good position tracking performance (Figs. 23-25), but with unsatisfactory control torques values, in the case of ordinary backstepping controller, particularly at the beginning of tracking (Fig. 25). Both torques of ordinary backstepping controller, for left and right wheels, exceed 50 Nm and they can produce the unnecessary actuators behavior. However, the hybrid controller ensures much less values of the control input torques for obtaining the reference position and orientation trajectories (Fig. 25). Consequently, the requested power of DC motors is also much less in the case of control by using the hybrid controller (Fig. 26).

4.2 Simulation results with fuzzy logic controller

The effectiveness of the fuzzy controller is demonstrated in the case of tracking of a more complex trajectory than lemniscate, such as trifolium curve. The simulation results obtained by fuzzy logic position controller are illustrated in Figs. 27-33. From figures 27-29, it can be concluded that satisfactory tracking results are obtained using this controller. Also, the fuzzy controller ensures much less values of the control input velocities (Fig. 30) than ordinary backstepping controller (Fig. 31) for obtaining the reference position and

orientation trajectories in comparison with the backstepping controller. Consequently the significant decreasing of wheel torques with fuzzy control is achieved (Figs. 32). The absolute torque values of both wheels not exceed 2 Nm. These values are 30-40 times less then torque values achieved with backstepping controller. The time response of wheel torques of ordinary backstepping controller is shown in Fig. 33.

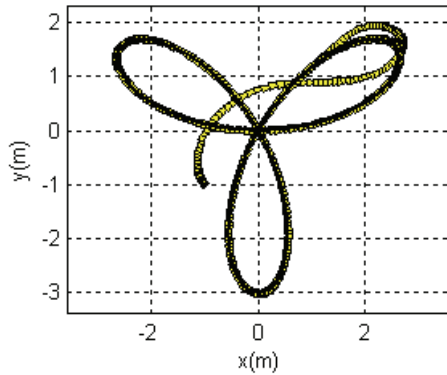


Figure 27. Tracking the trifolium trajectory

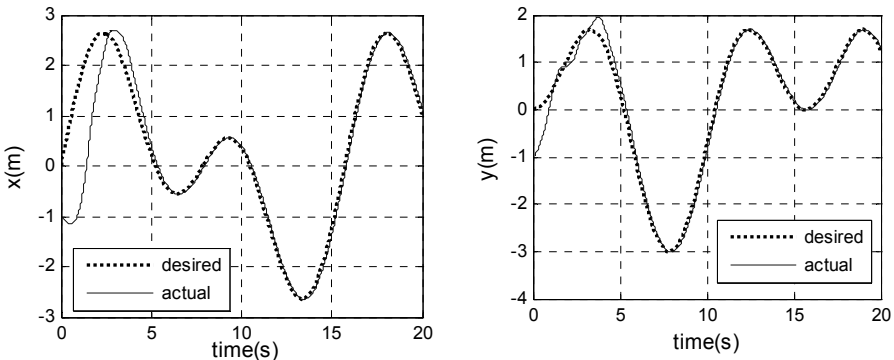


Figure 28. Time history of x and y coordinates

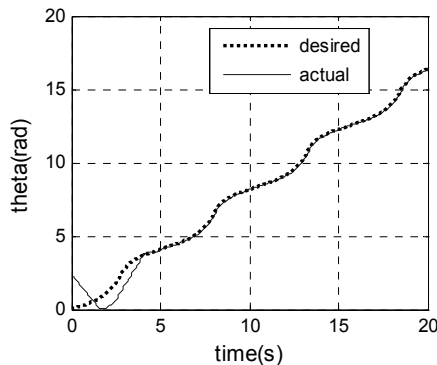


Figure 29. Orientation of the robot

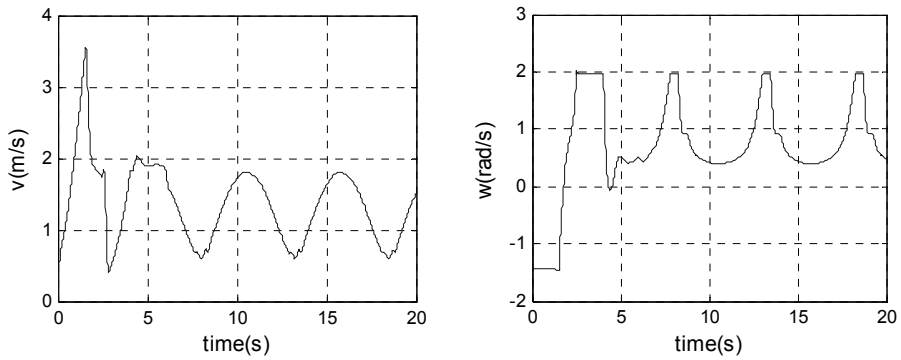


Figure 30. Linear (v) and angular (w) velocity outputs of fuzzy controller

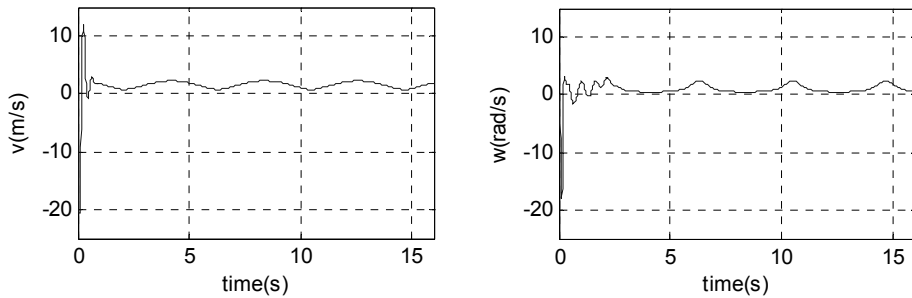


Figure 31. Linear (v) and angular (w) velocity outputs of ordinary backstepping controller

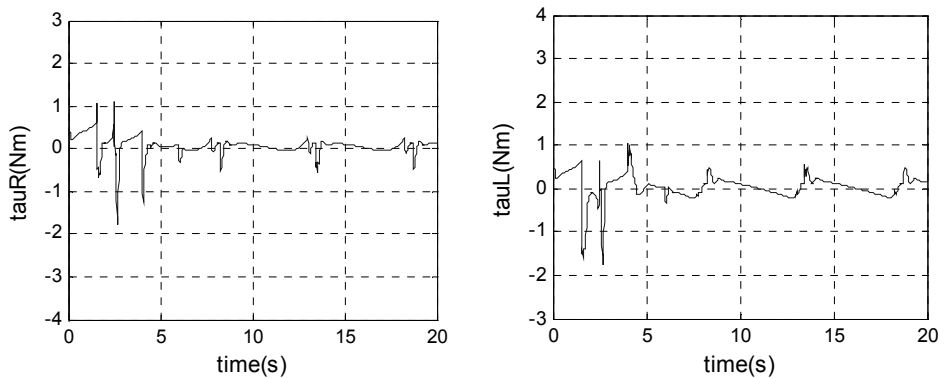


Figure 32. Right and left wheel torques of fuzzy

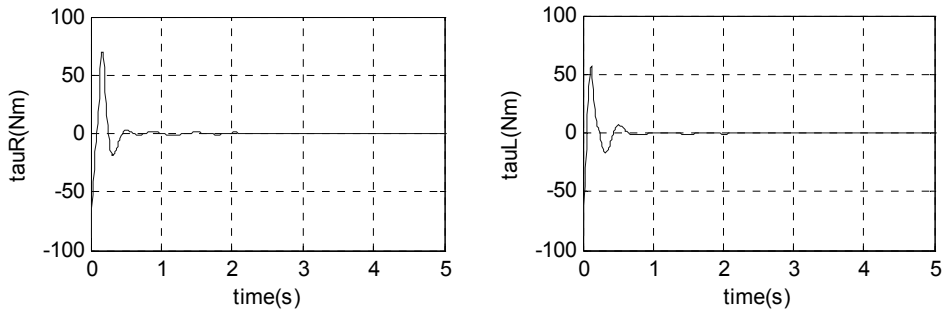


Figure 33. Right and left wheel torques of ordinary backstepping controller (first five seconds)

5. Conclusions

The experience of the design of the nonlinear position control confirmed the remarkable potential of backstepping and fuzzy logic in the development of effective decision laws capable of overcoming the inherent limitations of model-based control strategies. This paper focuses on design of hybrid backstepping and fuzzy position logic controls of mobile robot that satisfied a good position tracking performance with simultaneously satisfactory control of velocities, which has an impact on wheel torques. In our previously designed backstepping controller a good tracking performance was obtained. However, its main shortcoming is unsatisfactory control velocities values, particularly at the beginning of tracking. Control parameters of backstepping controller and membership functions of fuzzy controller are adjusted by genetic algorithms. Advantage of the proposed fuzzy controller, and also hybrid backstepping controller, lies in the fact that control velocities (and consequently, the control torques) cannot exceed certain limits. Consequently, these controllers radically decreased the control velocities without major impact on tracking performance. Finally, from the simulation results obtained, it can be concluded that the proposed hybrid backstepping and fuzzy design achieve the desired results. Future work will include the investigation of a fuzzy stability of the proposed fuzzy logic position system.

6. References

- Egerstedt, M.; Hu, X. & Stotsky, A. (2001). Control of Mobile Platforms Using a Virtual Vehicle Approach. *IEEE Transaction on Automatic Control*, Vol. 46, pp. 1777-1882
- Fierro, R. & Lewis, F. L. (1997). Control of a nonholonomic mobile robot: backstepping kinematics into dynamics. *Journal of Robotics Systems*, Vol. 14, No. 2, pp. 149-163.
- Fukao, T.; Nakagawa, H. & Adachi, N. (2000). Adaptive Tracking Control of a Nonholonomic Mobile Robot. *IEEE Transaction on Robotics and Automation*, Vol. 16, pp. 609-615.
- Hu, T. & Yang, S. X. (2001). Real-time Motion Control of a Nonholonomic Mobile Robot with Unknown Dynamics, Proceedings of the Computational Kinematics Conference, Seoul.

- Lacevic, B. & Velagic, J. (2005). Reduction of Control Torques of Mobile Robot Using Hybrid Nonlinear Position Controller, *Proceedings of the IEEE International Conference "Computer as a tool"*, pp. 161-166, Belgrade, November 2005.
- Lacevic, B. & Velagic, J. (2006). Stable Nonlinear Position Control Law for Mobile Robot Using Genetic Algorithm and Neural Networks, *Proceedings of the World Automation Congress, 6th International Symposium of Soft Computing for Industry (ISSCI)*, paper no. 50, Budapest, July 2006.
- Lacevic, B.; Velagic, J. & Osmic, N. (2007). Design of Fuzzy Logic Based Mobile Robot Position Controller Using Genetic Algorithm, *Proceedings of the Advanced Intelligent Mechatronics (AIM2007)*, pp. 1-6, Zurich, September 2007.
- Oriolo, G.; De Luca, A. & Vendittelli, M. (2002). WMR control via dynamic feedback linearization: design, implementation and experimental validation. *IEEE Transactions on Control System Technology*, Vol. 10, No. 6, pp. 835-852.
- Rajagopalan, R. & N. Barakat, N. (1997). Velocity Control of Wheeled Mobile Robots Using Computed Torque Control and Its Performance for a Differentially Driven Robot. *Journal of Robotic Systems*, Vol. 14, pp. 325-340.
- Tanner, H. G. & Kyriakopoulos, K. J. (2003). Backstepping for nonsmooth systems. *Automatica*, Vol. 39, pp. 1259-1265.
- Topalov, A. V.; Tsankova, D. D.; Petrov, M. G. & Proychev, Th. P. (1998). Intelligent Sensor-Based Navigation and Control of Mobile Robot in a Partially Known Environment, *Proceedings of the 3rd IFAC Symposium on Intelligent Autonomous Vehicles, IAV'98*, pp. 439-444, 1998.
- Velagic, J.; Lacevic, B. & Perunicic, B. New Concept of the Fast Reactive Mobile Robot Navigation Using a Pruning of Relevant Obstacles, *Proceedings of the IEEE International Symposium on Industrial Electronics (ISIE2005)*, pp. 161-166. Dubrovnik, June 2005.
- Velagic, J.; Lacevic, B. & Perunicic, B. (2006). A 3-Level Autonomous Mobile Robot Navigation System Designed by Using Reasoning/Search Approaches. *Robotics and Autonomous Systems*, Vol. 54, No. 12, pp. 989-1004.



Motion Planning

Edited by Xing-Jian Jing

ISBN 978-953-7619-01-5

Hard cover, 598 pages

Publisher InTech

Published online 01, June, 2008

Published in print edition June, 2008

In this book, new results or developments from different research backgrounds and application fields are put together to provide a wide and useful viewpoint on these headed research problems mentioned above, focused on the motion planning problem of mobile ro-bots. These results cover a large range of the problems that are frequently encountered in the motion planning of mobile robots both in theoretical methods and practical applications including obstacle avoidance methods, navigation and localization techniques, environmental modelling or map building methods, and vision signal processing etc. Different methods such as potential fields, reactive behaviours, neural-fuzzy based methods, motion control methods and so on are studied. Through this book and its references, the reader will definitely be able to get a thorough overview on the current research results for this specific topic in robotics. The book is intended for the readers who are interested and active in the field of robotics and especially for those who want to study and develop their own methods in motion/path planning or control for an intelligent robotic system.

How to reference

In order to correctly reference this scholarly work, feel free to copy and paste the following:

Jasmin Velagic, Bakir Lacevic and Nedim Osmic (2008). Nonlinear Motion Control of Mobile Robot Dynamic Model, Motion Planning, Xing-Jian Jing (Ed.), ISBN: 978-953-7619-01-5, InTech, Available from: http://www.intechopen.com/books/motion_planning/nonlinear_motion_control_of_mobile_robot_dynamic_model

INTECH
open science | open minds

InTech Europe

University Campus STeP Ri
Slavka Krautzeka 83/A
51000 Rijeka, Croatia
Phone: +385 (51) 770 447
Fax: +385 (51) 686 166
www.intechopen.com

InTech China

Unit 405, Office Block, Hotel Equatorial Shanghai
No.65, Yan An Road (West), Shanghai, 200040, China
中国上海市延安西路65号上海国际贵都大饭店办公楼405单元
Phone: +86-21-62489820
Fax: +86-21-62489821

© 2008 The Author(s). Licensee IntechOpen. This chapter is distributed under the terms of the [Creative Commons Attribution-NonCommercial-ShareAlike-3.0 License](#), which permits use, distribution and reproduction for non-commercial purposes, provided the original is properly cited and derivative works building on this content are distributed under the same license.